ELSEVIER

Journal of Materials Processing Technology 168 (2005) 360–366

Journal of Materials Processing Technology

www.elsevier.com/locate/jmatprotec

# Modelling of cold extrusion with experimental verification

P. Tiernan [a,*], M.T. Hillery [a], B. Draganescu [b], M. Gheorghe [b]

[a] *Manufacturing & Operations Engineering Department, University of Limerick, Limerick, Ireland, UK*
[b] *Faculty of Engineering and Management of Technological Systems, Polytechnic University of Bucharest, Romania*

Received 18 February 2004; received in revised form 2 January 2005; accepted 3 February 2005

**Abstract**

This paper reports on an experimental and finite element analysis (FEA) of the cold extrusion of high-grade (AA1100) aluminium. The influence of die angle, reduction ratio and die land on the extrusion force during the extrusion process was investigated. A forward extrusion die was designed and manufactured for the purpose of the experimental research. Interchangeable elements of the extrusion die allowed rapid change of the extrusion parameters to attain a high degree of experimental flexibility. A load cell, incorporated into the die design, allowed accurate determination of extrusion forces while a linear variable differential transformer (LVDT) provided automatic measurement of punch travel during the extrusion cycle. All data obtained from the instrumentation was captured and analysed using a personal computer (PC).

A finite element analysis (FEA) of the cold extrusion process was undertaken in parallel with the experimental programme. The FEA simulation was carried out using ELFEN, FEA software, specifically produced for metal forming simulation. An axisymmetrical 2D geometric model of the tooling and billet was constructed for the analysis. Data obtained from the FE model included die-work piece contact pressure, effective stress and strain and material deformation velocity. The correlation between the experimental, calculated and FEA data obtained in this research is presented and discussed.


*Keywords:* Forward extrusion; AA1100 aluminium; Extrusion force; Reduction ratio; Finite element analysis

## 1. Introduction

Extrusion, though one of the most important manufacturing processes today, is a relatively young metalworking process. Commercial extrusion of lead pipes started early in the 19th century and it was not until near the end of that century that it was possible to extrude even brass. This was largely because the heavy and sustained pressures necessary for extrusion were not available. In cold extrusion, which is used for the manufacture of special sections and hollow articles, the material is generally made to flow in the cold condition by the application of high pressure. The high pressures force the material through a cavity enclosed between a punch and a die. Cold extrusion can be used with any material that possesses adequate cold workability, e.g., tin, zinc, copper and its alloys, aluminium and its alloys. Indeed it is for these metals that the process is more widely adopted. Low-carbon soft annealed steel can also be cold extruded. If the product cannot be fully shaped in a single operation, the extrusion process may be performed in several stages [1]. The initial stock from which cold extrusions are produced consists of round blanks, lengths cut from bars, or specially preformed blanks.

The punches and dies used in cold extrusion are subjected to severe working conditions and are made of wear-resistant tool steels, e.g., high-alloy chromium steels. The main advantages of cold extrusion as opposed to hot extrusion are that good mechanical properties are imparted to the workpiece due to the severe cold working, good surface finish with the use of proper lubricants and no oxidation of the workpiece. Extrusion produces compressive and shear forces in the stock. No tensile force is produced, which makes high deformation possible without tearing the metal.

Previous research has shown that the extrusion die geometry, frictional conditions at the die–billet interface and thermal gradients within the billet greatly influence metal flow in cold extrusion [2]. Many researchers have attempted to investigate the effects of various lubricants at the die–billet

* Corresponding author.
*E-mail address:* peter.tiernan@ul.ie (P. Tiernan).

0924-0136/$ – see front matter © 2005 Elsevier B.V. All rights reserved.
doi:10.1016/j.jmatprotec.2005.02.249

interface. These investigations have resulted in a number of standard friction tests, e.g., ring and bucket test [3–5]. The influence of the friction at the die–billet interface on the geometrical accuracy of the extruded part has been investigated for the cold extrusion process using a finite element analysis. Various values for the coefficient of friction were used in finite element models. High values of the frictional coefficient produced greater form errors in the extruded component due to the greater compressive stresses at the contact surfaces of the die [6]. The influence of die half-angle and reduction ratio on extrusion force has been researched for the hydrostatic extrusion process and the data obtained can be used for the forward conventional extrusion process [7]. Geometrical characteristics of the extrusion die influence both the extrusion process and the mechanical properties of the extruded material. While it is widely acknowledged that one of the main effects of cold extrusion on the billet material is strain hardening, other mechanical characteristics of the extruded material also change. Using both experimental and finite element analysis, some researchers have analysed the hardness and density changes that occurred as a result of both the extrusion and drawing process [8]. Experimental investigations have been made to determine the effects of die reduction ratio, die angle and loading rate on the quality of cold extruded parts, extrusion pressures and flow patterns for both lead and aluminium [9]. Empirical equations were determined to assess the effect of the aforementioned extrusion variables on the extrusion pressure.

The geometrical features of the die land are a critical feature in obtaining defect free cold extruded parts. As the die land length directly influences the amount of friction at the die–billet interface, extrusion die designers use this geometrical parameter to control the metal flow from the die. Appropriate die land geometrical features will allow uniform distribution of residual stresses in the extruded part as it emerges from the die. Various proposals have been made by researchers to provide a numerical basis for the design of the die land parameter [10–12].

The ability of a crystalline material, particularly metals, to undergo plastic deformation rather than fracture is an invaluable property. Extruded and deformed products have undergone plastic deformation and this deformation increases their mechanical properties such as hardness and tensile strength. Generally, residual stresses exist within the part, which can only be relieved by an appropriate heat treatment process [13]. Furthermore, strength and hardness of the metal are increased with a corresponding loss in ductility as a result of a distortion or fragmentation of the grain structure. The occurrence of central bursts in cold extruded parts has been investigated as a function of die geometry [14]. These researchers concluded that the central bursts could be considered as the process of ductile fracture resulting from the coalescence and growth of microvoids in the materials. The basic idea of many ductile fracture criteria is that fracture occurs when the value of a damage parameter reaches a critical value [15–18].

The relationship between extrusion velocity with both temperature distribution within the extruded part and extrusion load has been investigated by a number of researchers [19–23]. The extrusion load was shown to increase with extrusion velocity. The magnitude of the increase is larger at higher reduction ratios.

## 2. Aims of research

An experimental programme of forward cold extrusion was undertaken in the present investigation. The aims of the research were to analyse the effect of three geometrical variables, namely, reduction ratio, die angle and die land height on the extrusion force. Experiments were conducted using two different lubricants; zinc stearate and an oil-based lubricant that contained lead and copper additives. The magnitude of the extrusion force was determined experimentally by means of a force transducer. The data obtained from these measurements was compared to data obtained by calculation using a previously published theoretical formula and from finite element software predictions. Fifteen experiments were carried out using various die geometries with both lubricants.

## 3. Experimental research

### 3.1. Billet preparation

The billets, of initial diameter and height, 38 and 20 mm, respectively had a chemical composition as presented in Table 1. The billets were subjected to an annealing treatment to eliminate any residual stresses present prior to extrusion. This consisted of heating the billets to 345 °C in an induction oven, soaking at this temperature for 15 min, followed by gradually cooling in air to room temperature.

### 3.2. Extrusion tool design

An extrusion tool was designed and manufactured for the experimental programme. It consisted mainly, of three main

Table 1
Chemical composition (wt%) of the billet material

| | |
|---|---|
| Si | – |
| Fe | 0.19 |
| Cu | 0.008 |
| Mn | 0.02 |
| Mg | 0.058 |
| Cr | 0.006 |
| Ni | 0.001 |
| Zn | 0.001 |
| Ga | – |
| V | – |
| Ti | – |
| Al | 99.71 |

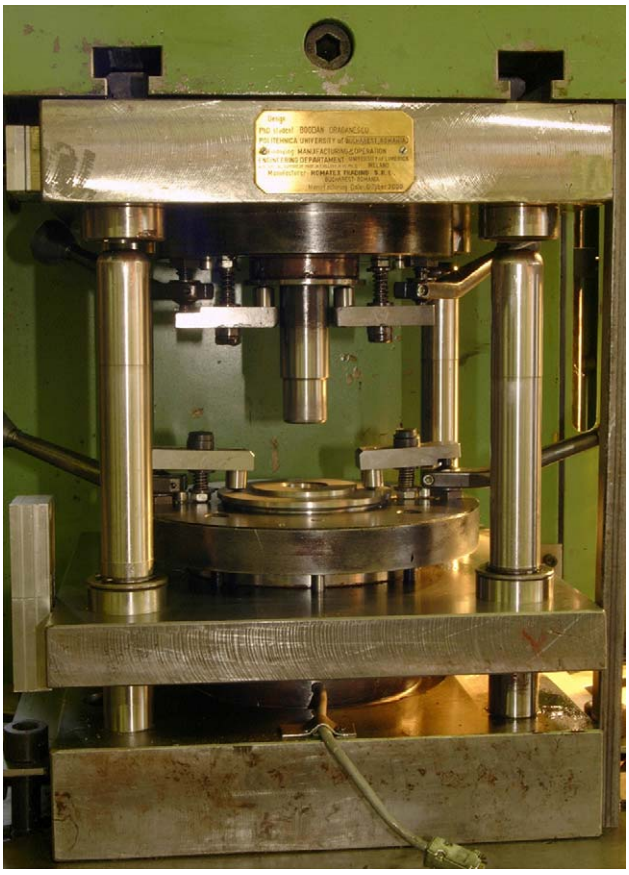

Fig. 1. Extrusion die.

plates: upper, active and lower. The upper and active plates were free to move on four pillars as shown in Fig. 1. A rapid punch and die release system was incorporated into the overall tool design to facilitate reduced experiment set up times and allow a high degree of experimental flexibility. The extrusion force was transmitted from the active die through a pressure plate to the force transducer. The contact surface between the pressure plate and the force transducer was machined to a hemispherical form to eliminate any force components in the horizontal direction. The force-sensing component was designed for a nominal load of 2 MN. This load, $F$, was calculated using a modified upper bound equation, i.e., Equation (1) [24]:

$$F = 2k_{\mathrm{f}}\left[4\mu\cdot\left(\frac{H}{D}+\frac{h}{d}\right)+\left(\frac{\mu}{\sin\alpha}+1\right)\cdot\ln\frac{D^2}{d^2}\right]\times\frac{\pi\cdot D^2}{4} \quad (1)$$

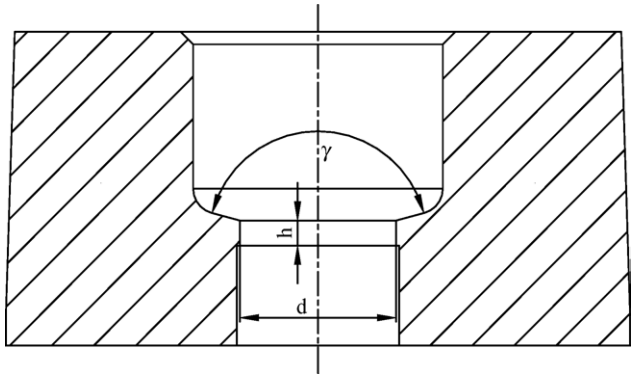


Fig. 2. Extrusion die geometry.

where $\mu$ is the coefficient of friction at die/billet interface, $D$ the billet diameter (mm); $d$ the die land diameter (mm), $h$ the Die land height (mm), $a$ the die half angle (°), $H$ the billet height (mm) and $k_{\mathrm{f}}$ is the maximum tangential stress at die–billet interface (N/mm$^2$).

Strain gauges were mounted on the force-sensing component and connected to form a wheatstone bridge circuit. An optimum mounting position for bonding the strain gauges was established by modelling the elastic deformation of the transducer with ANSYS finite element software. The load cell was mounted in the extrusion die and calibrated using a high precision calibration device. An LVDT transducer was attached between the top plate and the active plate of the extrusion die to monitor punch travel. The output signals from the strain gauges and LVDT were amplified and filtered using a signal-conditioning unit.

### 3.3. Experimental programme

The experimental program undertaken is outlined in Table 2. The three parameters varied during the experimental work were the die exit diameter, $d$, die land height, $h$ and die angle, $\gamma$. The die geometry is shown in Fig. 2.

## 4. Finite element analysis

A mechanical simulation of the extrusion process was performed using the finite element software. This was achieved by constructing an accurate two-dimensional CAD model of the process. The model was meshed with appropriate elements and material properties and boundary conditions were added. As the meshed model became distorted during the simulation, remeshing facility made the analysis of large de-

Table 2
Experimental programme

| Experiment No. | 1 | 2 | 3 | 4 | 5 | 6 | 7 | 8 | 9 | 10 | 11 | 12 | 13 | 14 | 15 |
|---|---|---|---|---|---|---|---|---|---|---|---|---|---|---|---|
| $d$ (mm) | 9 | 21 | 9 | 21 | 9 | 21 | 9 | 21 | 5 | 25 | 15 | 15 | 15 | 15 | 15 |
| $h$ (mm) | 2.8 | 2.8 | 5.2 | 5.2 | 2.8 | 2.8 | 5.2 | 5.2 | 4 | 4 | 2 | 6 | 4 | 4 | 4 |
| $\gamma$ (°) | 132 | 132 | 132 | 132 | 168 | 168 | 168 | 168 | 150 | 150 | 150 | 150 | 120 | 180 | 150 |

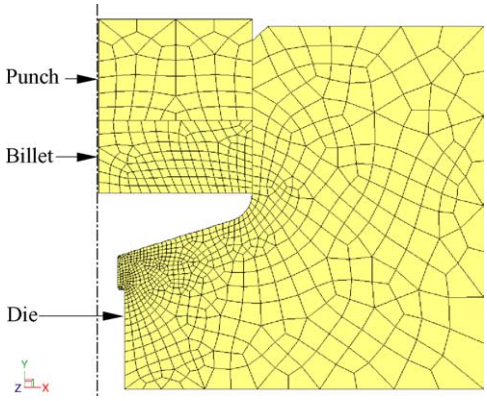


Fig. 3. Finite element model of extrusion process.

formations and strains possible. The complete meshed model of the extrusion process is shown in Fig. 3.

### 4.1. FEA formulation

ELFEN/explicit, a dynamic explicit finite element code, was used to perform the simulation. The flow formulation approach, using rigid plastic material elements, was used in the finite element analysis. The constitutive equations for this approach are identical to those for a non-Newtonian fluid. Nodal velocities defined in the Eulerian mesh were the unknowns in the flow formulation and were related to the material strain rates by standard kinematical expressions. Using this method it was possible to calculate the deformation power as a product of the invariants of the stress and strain rate tensors, which makes the solution insensitive to rotations. In the Eulerian formulation the material flows through a frame of reference, which is fixed in space. Therefore, problems with grid distortion due to large deformation are eliminated.

As the material boundaries do not follow the mesh lines in a Eulerian calculation, the mesh generation is completely independent of the structure, which greatly simplifies both the mesh generation and the structure definition. The Eulerian formulation used in the present work is based on operator splitting, which permits the sequential solution in two steps of the Eulerian conservation equations, i.e., Equation Set (2):

$$\frac{\partial \rho}{\partial t} + \nabla \cdot (\rho u) = 0;$$
$$\frac{\partial \rho u}{\partial t} + \nabla \cdot (\rho u \otimes u) = \nabla \cdot \sigma + \rho b;$$
$$\frac{\partial \rho e}{\partial t} + \nabla \cdot (\rho e u) = \sigma : \dot{\varepsilon} \quad (2)$$

where $\rho$ is the density, $\mu$ the velocity, $\sigma$ the Cauchy stress tensor, $\dot{\varepsilon}$ the strain rate tensor, $b$ the body force and $e$ is the internal energy.

The non-linear behaviour of the billet material, i.e., the material hardening was accounted for using the Von Mises criterion. Stress–strain data for the AA1100 material was obtained from previously published work [25]. The A1100 aluminium was modelled as a viscoplastic material while the punch and die elements were modelled with elastic elements.

## 5. Results

On completion of the FE simulations billet–die interface contact pressure, effective stress and strain and material de-

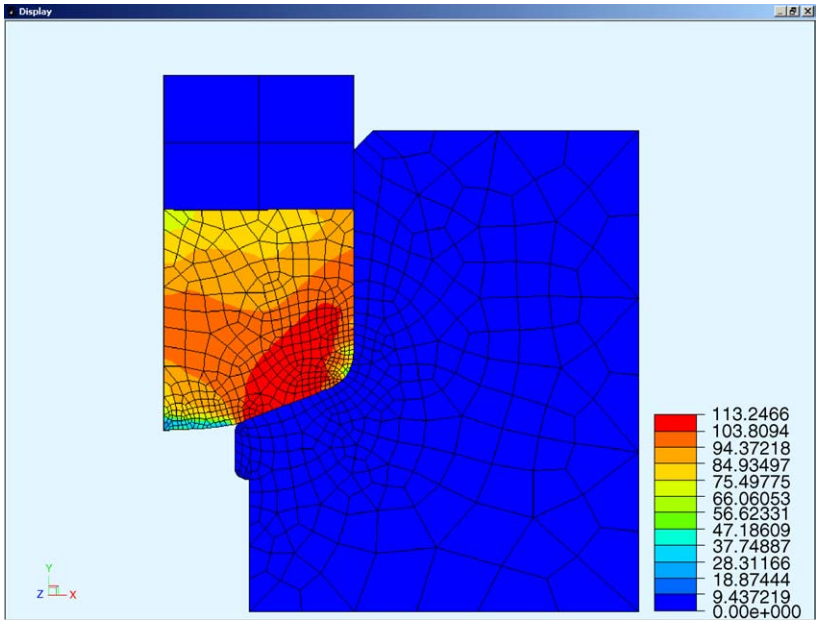


Fig. 4. Billet stress contours as metal begins to flow through die (MPa).

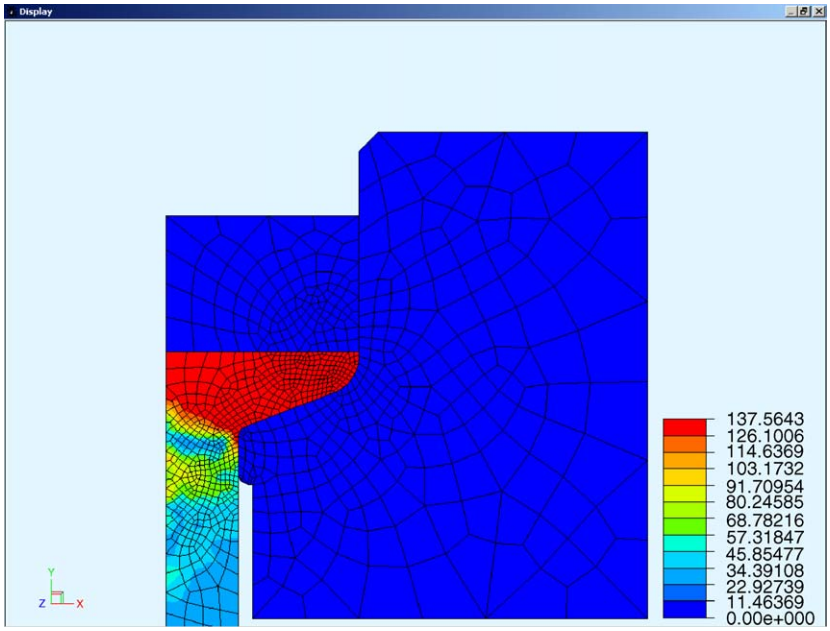


Fig. 5. Billet stress contours at end of extrusion process (MPa).

formation velocities were output to file. The effective stress distribution within the billet at various stages of the extrusion process is presented in Figs. 4 and 5.

Values for maximum extrusion forces were obtained from the finite element simulation by high-resolution history plots. This function was programmed in the post analysis module of the software. An example of such an output is presented in Fig. 6.

The magnitude of the extrusion force obtained from the FE simulation was compared to values acquired by both experiment and calculation. This comparison is presented in Table 3 and graphically displayed in Figs. 7 and 8. The calculated values were obtained from Equation (1).

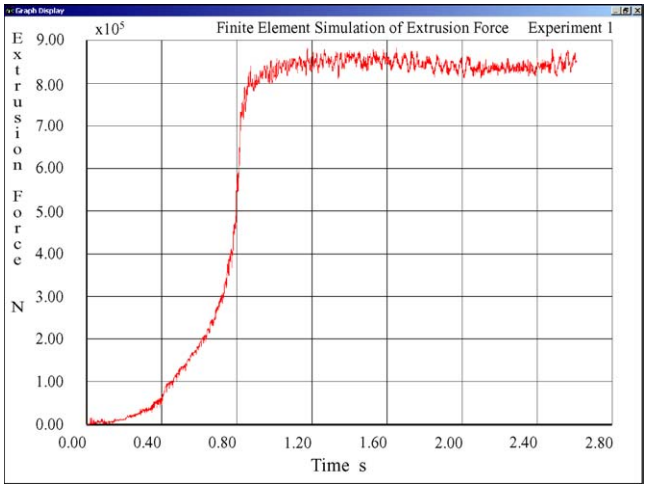


Fig. 6. High-resolution history plot of extrusion for Experiment No. 1.

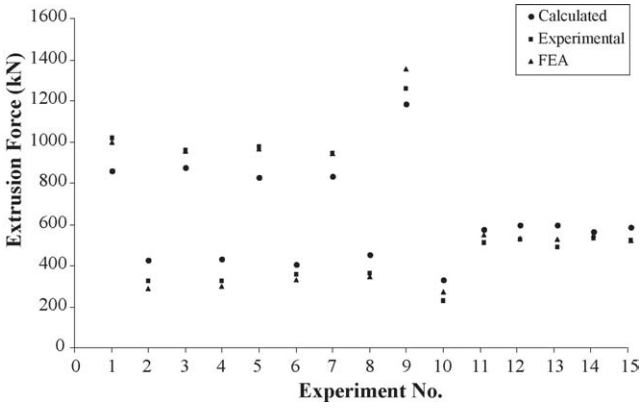


Fig. 7. Extrusion force using Zn Stearate lubricant.

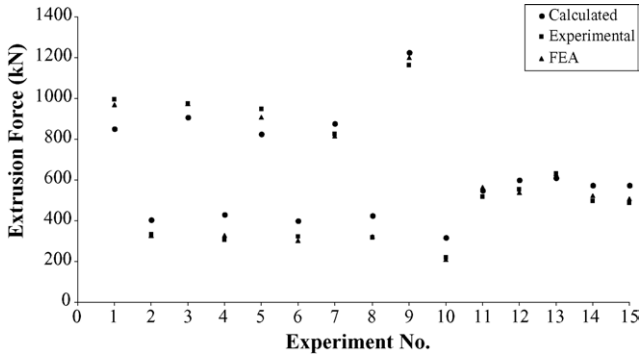


Fig. 8. Extrusion force using Cu–Pb lubricant.

Table 3
Maximum extrusion force (kN)

| Experiment No. | Zn sterate lubricant | | | Cu–Pb lubricant | | |
|---|---|---|---|---|---|---|
| | Calculated | Experimental | FEA | Calculated | Experimental | FEA |
| 1 | 856.41 | 1016.01 | 995.78 | 851.6 | 994.17 | 969.29 |
| 2 | 425.49 | 323.24 | 286.75 | 407.1 | 331.63 | 326.93 |
| 3 | 876.38 | 961.57 | 954.65 | 905.3 | 975.32 | 975.99 |
| 4 | 430.49 | 323.24 | 300.07 | 430.1 | 309.66 | 330.51 |
| 5 | 826.86 | 977.87 | 965.71 | 825.7 | 947.99 | 909.42 |
| 6 | 406.8 | 358.55 | 330.14 | 401.3 | 321.37 | 302.99 |
| 7 | 830.89 | 945.24 | 946.4 | 879.3 | 827.2 | 814.18 |
| 8 | 451.84 | 361.27 | 346.17 | 424.3 | 317.78 | 324.95 |
| 9 | 1186.2 | 1260.27 | 1356.5 | 1226 | 1164.71 | 1202.31 |
| 10 | 330.55 | 228.17 | 273.42 | 320.4 | 220.02 | 209.18 |
| 11 | 575.13 | 509.95 | 548.96 | 548.4 | 518.82 | 562.49 |
| 12 | 595.84 | 526.96 | 536 | 602.1 | 553.88 | 536.23 |
| 13 | 597.08 | 492.08 | 527.51 | 612.2 | 632.9 | 629.86 |
| 14 | 563.88 | 532.78 | 548.83 | 571.8 | 495.4 | 525.2 |
| 15 | 586.4 | 521.37 | 521.37 | 575.2 | 488.72 | 505.85 |

## 6. Discussion

Fifteen manufactured die sets were successfully used in a purpose built extrusion tool to investigate the effect of die geometry on the extrusion force. It was possible to vary the reduction ratio between 60% and 98.4% and vary the die angle from 120° to 180°. Additionally the die land was varied from 2 to 6 mm. Two lubricants were used during the extrusion experiments. A finite element analysis of the extrusion process was carried out in parallel to the experimental programme. The high-grade aluminium billet was modelled as a perfect plastic material for the non-linear analysis during the finite element simulation. Output from the finite element program included extrusion force, effective stress and strain and material deformation velocities.

From Table 3, it is evident that the maximum extrusion force obtained corresponds to Experiment No. 9. The die exit diameter, angle and land height for this experiment were 5mm, 150° and 4 mm, respectively. This experiment represented the largest percentage reduction in the extrusion experiments and consequently required the largest force to successfully extrude the aluminium. Further investigation of Table 3 and Figs. 7 and 8 show that the extrusion force is a function of die angle. Experiments Nos. 1 and 5, utilised dies with die angles of 132° and 168°, respectively, while the die exit diameter and die land height were constant. Extrusion loads of 1016.01 and 977.87 kN were obtained experimentally using the Zn sterate lubricant for Experiments Nos. 1 and 5, respectively. A similar trend was found for Experiment Nos. 13, 14 and 15. These results indicate that as the die angle is reduced, larger extrusion forces are required to extrude aluminium AA1100. This is due to the increased contact length between the die and the billet leading to high friction power losses. Further research will establish an optimum die angle for the process. On examination of the extrusion load as a function of die land length, it is evident that the extrusion force required increased as the die land increased. From Table 3, in Experiment Nos. 11, 12 and 15, both the die exit diameter and the die angle are constant. As the land length is increased, there is a corresponding increase in the extrusion force. Dies with land lengths of 2, 4 and 6 mm were used in Experiment Nos. 11, 15 and 12, respectively. The corresponding loads obtained from experiment, FEA and calculation show an increase as land length increased. For die land lengths of 2, 4 and 6 mm; extrusion forces of 575.13, 586.4 and 595.84 kN were found by experiment, respectively.

The stress distribution at two stages of the extrusion process for Experiment No. 12 is presented in Figs. 4 and 5. The maximum stress value shown in Fig. 5 is 137.5 MPa. This level of stress occurs in the billet at the die angle as the metal exits the die. High-resolution plots were obtained from the finite element software to enable determination of extrusion forces. An example of such a plot is shown in Fig. 6. This graph shows an extrusion force of 856.4 kN was required when using a die with included angle, exit diameter and land height of 132°, 9 and 2.8 mm, respectively.

The FE model did not account for thermal softening of the billet or variations in the frictional coefficient at the billet–die interface due to lubricant breakdown. The maximum percentage error noted when the experimental value was compared to the FEA prediction was 8.42%. On comparing values of extrusion forces obtained from the FE software and those obtained by calculation, the most significant errors occurred at the smallest reduction ratios, i.e., Experiment Nos. 2, 4, 6, 8 and 10. Nevertheless at higher reduction ratios, i.e, where the die exit diameter is 9 and 5 mm, the FEA prediction error is below 11%.

The main reasons for differences in the FEA and experimental results can be attributed to frictional and deformation heating of the extruded material, unstable die–billet interface conditions and measurement errors.

## 7. Conclusions

A successful experimental programme of cold extrusion of high-grade (AA1100) aluminium was carried out with purpose-built tooling. Extrusion forces were successfully determined by incorporation of a load cell in the tooling set-up. Experiments were conducted using two different lubricants; zinc stearate and an oil-based lubricant that contained high pressure lead and copper additives. There was no remarkable difference in the extrusion forces required for the different lubricants. The finite element results show good correlation with results obtained from the experimentation, thus confirming the accuracy of the finite element model.

Furthermore extrusion force data obtained by calculation show reasonable agreement with data obtained from both calculation and FE work. The largest extrusion force obtained by experiment was 1260 kN. This force was measured when extruding the aluminium billet using a die with exit diameter, die angle, and land height of 5 mm, 150° and 4 mm, respectively. This represents a reduction in area of the billet of 98.2%. Further research is planned to quantify the effect the extrusion process has on the hardness and surface roughness of the extruded component. The values for the magnitude of the extrusion forces obtained experimentally were compared to both the finite element results and data calculated from Eq. (1). This comparison of results is illustrated in Table 3 and Figs. 7 and 8. Reasonable correlation exists between the FE, experimental and calculated values of the extrusion force.

Although a satisfactory accuracy was obtained in predicting the extrusion loads for certain experiments, it is evident the FE model would benefit from further refinement to enable precisely simulation the extrusion process characteristics.

## References

[1] G.W. Rowe, Principle of Principles of Industrial Metalworking Processes, Arnold, London, 1977.
[2] T. Altan, S.I. Oh, H. Gegel, Metal Forming; Fundamentals and Applications, American Society for Metals, Metals Park, Ohio, 1983.
[3] C.H. Lee, T. Altan, Influence of flow stress and friction upon metal flow in upset forging of rings and cylinders, J. Eng. Ind. 94 (1972) 775–782.
[4] G. Shen, A. Vedhanayagam, E. Kropp, T. Altan, A method for evaluating friction using a backward extrusion-type forging, J. Mater. Process. Technol. 33 (1992) 109, Elsevier.
[5] L. Lazzarotto, L. Dubar, A. Dubois, P. Ravassard, J. Oudin, Three selection criteria for the cold metal forming lubricating oils containing extreme pressure agents, J. Mater. Process. Technol. 80-81 (1998) 245–250, Elsevier.
[6] H. Long, R. Balendra, FE simulation of the influence of thermal and elastic effects on the accuracy of cold extruded components, J. Mater. Proc. Tech. 84 (1998) 247–260, Elsevier.
[7] A.H. Elkholy, Parametric optimisation of power in hydrostatic extrusion, J. Mater. Process. Technol. 70 (1997) 111–115, Elsevier.
[8] Y.S. Lee, S.Y. Hanm, Mechanical Property Changes in Drawing/Extrusion of Hardening Viscoplastic Materials With Damage, Int. J. Mech. Sci. 39 (5) (1997) 567–573.
[9] S.O. Onuh, M. Ekoja, M.B. Adeyemi, Effects of die geometry and extrusion speed on the cold extrusion of aluminium and lead alloys, J. Mater. Proc. Tech. 132 (2002) 274–285, Elsevier.
[10] H. Nanhai, L. Kezhi, Numerical design of the die land for shape extrusion, J. Mater. Proc. Tech. 101 (2000) 81–84.
[11] N. Miles, G. Evans, A. Middleditch, Bearing lengths for extrusion dies, rationale, current practice and requirements for automation, J. Mater. Proc. Tech. 72 (1997) 162–176.
[12] T. Chanda, J. Zhou, J. Duszczyk, FEM analysis of aluminium extrusion through square and round dies, Mater. Des. 21 (2000) 323–335.
[13] A. Pyzalla, W. Reimers, Residual-stresses and texture in cold forward extrusion, in: Proceedings of the International Conference on Competitive Advantage by Near-net-shape Manufacture, 1997, pp. 175–180 (Chapter 38).
[14] Ko Dae-Cheol, Kim Byung-Min, The prediction of central burst defects in extrusion and wire drawing, J. Mat. Proc. Technol. 102 (2000) 19–24, Elsevier.
[15] F.A. McClintock, A criterion for ductile criterion by the growth of holes, J. Appl. Mech. 35 (1968) 363–371.
[16] M. Oyane, T. Sato, K. Okimoto, S. Shima, Criteria of ductile fracture and their application, J. Mech. Work. Technol. 4 (1980) 65–81.
[17] M.G. Cockcroft, D.J. Latham, Ductility and the workability of metals, J. Inst. Met. 96 (1968) 33–39.
[18] K. Osakada, K. Mori, Prediction of ductile fracture in cold forging, Ann. CIRP 27 1 (1978) 135–139.
[19] T. Altan, S. Kobayashi, A numerical method for estimating the temperature distribution in extrusion through conical dies, J. Eng. Ind. 90 (1968) 107.
[20] P.K. Saha, R.K. Gosh, Temperature distribution during hot extrusion of aluminium—theoretical evaluation, Indian J. Technol. 17 (1979) 88–96.
[21] A.F. Castle, T. Sheppard, Hot working theory applied to extrusion of some aluminium alloys, Met. Technol. 3 (10) (1976) 42.
[22] P.K. Saha, Thermodynamics and tribology in aluminium extrusion, Wear 218 (1998) 179–190, Elsevier.
[23] T.J. Ward, R.M. Kelly, G.A. Jones, J.F. Heffron, The effects of nitrogen – liquid and gaseous – on aluminium extrusion productivity, J. Met. (December) (1984) 28.
[24] I. Tapalaga, et al., Cold Extrusion of Metals, Dacia, Cluj-Napoca, Romania, 1986.
[25] P.E. Armstrong, J.E. Hockett, O.D. Sherby, Large strain-multidirectional deformation of 1100 aluminium at 300K, J. Mech. Phys. Solids 30 (1–2) (1982) 132.